Int J Clin Exp Med 2016;9(3):5439-5448
www.ijcem.com /ISSN:1940-5901/IJCEM0019070

Original Article

Reversal of doxorubicin-resistance by delivering tetramethylprazine via folate-chitosan nanoparticles in MCF-7/ADM cells

Hui Ma[1*], Chenxin Deng[1*], Xingyue Zong[2*], Yufang He[1*], Lichun Cheng[1*], Qing Fan[1], Mingkun Shao[1], Yuan Lin[3], Chenyang Zhao[1], Guiru Li[1], Ce Zhang[1]

[1]Department of Pharmacy, The Second Hospital of Dalian Medical University, Dalian 116027, China; [2]Medical Sciences Program, Indiana University School of Medicine, Bloomington, Indiana, USA; [3]College of Pharmacy, Dalian Medical University, Dalian 116044, China. [*]Equal contributors.

Received November 3, 2015; Accepted February 25, 2016; Epub March 15, 2016; Published March 30, 2016

Abstract: Multidrug resistance (MDR) is a current challenge for cancer therapy. Tetramethylprazine (TMP) has been shown to reverse MDR to several anti-cancer drugs, but the lack of appropriate carrier and a short half-life limits its clinical application. In this study, we developed folate-chitosan nanoparticles loaded with TMP (FA-TMP-NP) to improve the sensitivity of MDR cells to chemotherapy. MCF-7/ADM cells with high folate receptor expression and K562/ADM cells with low folate receptor expression are treated with FA-TMP-NP and adriamycin (ADM), using chitosan nanoparticles loaded with TMP (CS-TMP-NP) and TMP solution as control. We determined the cytotoxicity by MTT assay, ADM accumulation by flow cytometer and laser scanning confocal microscope, and intracellular ADM concentrations by fluorescence spectrophotography. We analyzed the protein levels of P-glycoprotein (P-gp) and glutathione S-transferases-π (GST-π) by Western blotting and the mRNA levels of MDR-1 and GST-π by real-time PCR. Compared with the control preparations, FA-TMP-NP significantly enhanced the ADM fluorescence intensity and increased the intracellular concentrations of ADM in MCF-7/ADM cells in a dose-dependent and time-dependent manner, accompanied with decreased P-gp and GST-π. In contrast, there was no significant difference between FA-TMP-NP and control preparations in K562/ADM cells. Our results indicate that FA-TMP-NP is a novel drug delivery system, which could improve the specificity of tumor cells with high folate receptor expression to chemotherapy, suggesting promising further development as a reversal agent for MDR.

Keywords: Folate-chitosan nanoparticles, folate receptor, tetramethylprazine, MCF-7/ADM, MDR reversal

Introduction

Multi-drug resistance (MDR) is an indispensable factor leading to the failure of cancer chemotherapy. MDR can act through either transporter-based or non-transporter-based processes [1], in which transporter-based delivery process is mainly concerned with ATP binding cassette (ABC) transporters [2, 3]. Some typical ABC transporters are p-glycoprotein (P-gp), breast cancer resistance protein (BCRP), lung resistance-related protein (LRP), and multidrug resistance protein (MRP) [4]. These cell membrane transport proteins pump the cytotoxic drugs out of cells through active transportation. Increased expressions of these proteins in cancer cells causes reduced intracellular drug concentration. Among these proteins, P-gp is overexpressed in the majority of cancer cells, and most lipid-soluble chemotherapeutic drugs are its substrates including doxorubicin, paclitaxel [5], and Vincristine [6]. Thus, P-gp and its gene coding MDR-1, is a widely used biomarker for MDR and the most attractive target for the study of MDR reversal agent. Non-transporter-based MDR, on the other hand, acts by altering the activities of cellular enzymes such as glutathione S-transferases (GSTs). GSTs play an important role in the development of drug resistance through detoxification. GST-π, a cytosolic isoform of GSTs, has the closest relationship with cancer progression and is overexpressed in most drug-resistant cancer cell lines. GST-π

catalyzes the conjugation of glutathione with chemotherapeutic drugs, thereby facilitating the excretion of various potential toxic chemicals, carcinogenic agents and lipophilic compounds via increasing their water-solubility or binding. It can mediate MDR of cancer cells to various anti-tumor drugs including platinum and alkylating agent. It has been found that GST-π inhibitors suppress MDR and sensitize cancer cells to chemotherapeutic agents [5, 7, 8]. Therefore, GST-π is another biomarker for MDR.

Tetramethylprazine (TMP, 2,3,5,6-tetramethylpyrazine) is an alkaloid monomer extracted from Umbelliferae Chuanxiong rhizome [9, 10]. Accumulating data have shown that TMP plays a significant role in reversing MDR [8, 11, 12]. TMP has been shown to sensitize tumor MDR cells to chemotherapeutic drugs, such as doxorubicin and cisplatin, by down-regulating the expression of P-gp, thereby increasing the intracellular concentration of chemotherapeutic drugs [13, 14]. However, its clinical application as a reversal agent is very limited, probably due to the facts that TMP is easy to be oxidized and its in vivo half-life is approximately 1.5 h. Moreover, the traditional formulation of TMP has the problems of excessive dosing frequency, wide in vivo distribution range, low drug concentration at target site, and inconvenient combination usage with chemotherapeutic drugs. In addition, reports in recent years suggest that the injection form of TMP causes relatively high frequency of adverse reactions, including toxic side-effects in respiratory, nervous and reproductive system. As a result, all existing preparations of TMP are not suitable for its application in reversing MDR in cancer. In order to reach the goal of targeting delivery, we developed folate modified chitosan nanoparticles loaded with TMP (FA-TMP-NP). Folate receptor (FR) is overexpressed in many types of cancer cells [15], including cervical, breast, brain, lung, and kidney cancer cells. Therefore, FA-TMP-NP may target to folate receptors in an active targeting manner and enable accumulation and release of nanoparticles in specific tumor tissues via endocytosis process mediated by folate receptors.

In this study, we choose drug-resistant human breast cancer cell MCF-7/ADM and its sensitive line MCF-7 as experimental models, both of which overexpress folate receptors. At the same time, we used drug-resistant human leukemia K562/ADM cells and its sensitive line with low folate receptor expression as controls. Currently, the mechanism study about the reversal of MDR by is mainly focusing on MDR gene and its coding protein P-gp. However, the mechanism study on other proteins or non-transporter-based processes is very rare [11]. According to literature and our preliminary study, we focused on P-gp and GST-π in the present study. So the reversing MDR Mechanism can be further explain the way from multiple perspectives and multiple targets, furthermore new ideas are provided in promoting natural drug TMP applications.

Materials and methods

Materials

For the preparation of nanoparticle formulations, folate-chitosan (50 kDa, lot number: 20120501) was synthesized in the pharmacy lab of the Second Hospital of Dalian Medical University. Tetramethylprazine (TMP, 2,3,5,6-tetramethylpyrazine) was obtained from Ze Lang Pharmaceutical (Nanjing, China). Sodium polyphosphate (TPP) was supplied by Kermel Chemical Reagent (Tianjin, China) and used as anion agent. Adriamycin (ADM) was obtained from Pfizer Pharmaceutical (San Diego, CA, USA). Verapamil injection was from Shanghai Hefeng Pharmaceutical (Shanghai, China). IP cracking liquid was purchased from Beyotime Institute of Biotechnology (Shanghai, China). Rabbit anti-human P-gp and rat anti-human GST-π antibodies were supplied by Abcam Biotechnology (Cambridge, MA, USA). RNAiso plus, SYBR® Premix Ex Taq™ and PrimeScript® RT reagent Kit with gDNA Eraser were from Dalian Takara BIO (Dalian, China).

Preparation and characterization of FA-TMP-NP

The preparation of FA-TMP-NP or CS-TMP-NP was based on ionic cross-linking technique. Briefly, folate-chitosan or chitosan was added into 1% (w/w) acetic acid (pH 5.0) to make the final concentration of 2 mg/ml and mixed with TMP. Then TPP was dissolved in distilled water to a concentration of 1 mg/ml. Subsequently, TPP solution was added dropwise into the mix-

Table 1. Primer sequences for real-time PCR

Gene	Forwards	Reverse
MDR 1	AGGCCAACATACATGCCTTCATC	GCTGACGTGGCTTCATCCAA
GST-π	TCCGCTGCAAATACATCTCC	TGTTTCCCGTTGCCATTGAT
β-actin	TGGCACCCAGCACAATGA A	CTAAGTCATAGTCCGCCTAGAAGCA

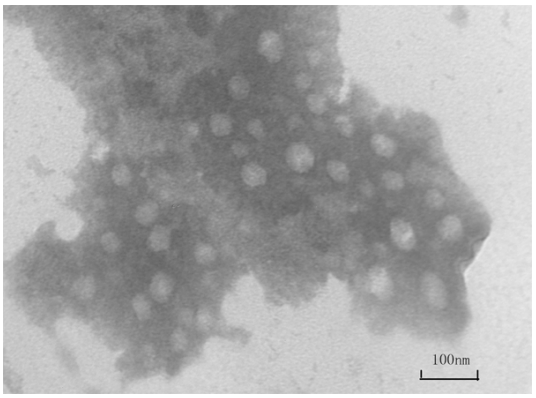

Figure 1. Transmission electronic micrograph of FA-CS-TMP-NPs. Scale bar =100 nm. FA-CS-TMP-NPs have uniform spherical morphology.

ture and kept continuously stirring at room temperature for 1 h. Then the product was centrifuged at 100,000 g for 30 min, and the supernatant is collected for further encapsulation efficiency (EE) and loading efficiency (LE) analysis. The precipitation was dissolved in water and isolated by lyophilization. The obtained nanoparticles were viewed under transmission electron microscope (TEM, JEM-2000EX, JEOL Co. Japan). EE and LE of FA-TMP-NP was analyzed by HPLC with programmable solvent module 125 (Beckman, USA). The particle size and Zeta potential were determined using dynamic light scattering (Malvern Instruments, UK).

Cell culture

Human breast carcinoma cell line MCF-7 and its multidrug resistance sub-line, MCF-7/ADM, were purchased from KeyGen biotech (Nanjing, China). Human leukemia cells K562 and its multidrug resistance subline, K562/ADM, were purchased from Blood Research Administration (Tianjin, China). All the cell lines were cultured in RPMI1640 medium containing 10% fetal bovine serum (FBS), 100 U·mL-1 penicillin, and 100 μg·mL^{-1} of streptomycin at 37°C humid atmosphere with 5% CO_2. To maintain the level of resistance, MCF-7/ADM and K562/ADM cells were cultured in medium containing 1 μg·mL^{-1} ADM at least one week prior to use.

Cytotoxicity assay

MCF-7/ADM and K562/ADM cells were seeded at a density of 1×10^5 mL^{-1} in 96-well plates, and treated with different concentrations of FA-TMP-NP ranging from 31 μg·mL^{-1} to 1000 μg·mL^{-1}. After treatment for 24, 48, 72 h, 0.5% MTT (Sigma, America) solution was added to each well and incubated for another 4 h. Then 100 μL DMSO was added into each well and the absorbance was detected with microplate reader (Thermo 354, USA) at 492 nm. The cell viability was calculated as (OD treated group/OD control group) ×100%. After treatment for 24 h, we calculated IC_{95}, IC_{85} and IC_{80}.

Determination of MDR reversal activity

MCF-7/ADM, MCF-7, K562/ADM and K562 cells were seeded at a density of 1×10^5 mL^{-1} in 96-well plates. ADM of 0.5 μg·mL^{-1} was added in the cells alone, or in combination with reversal agent FA-TMP-NP (IC_{95}), CS-TMP-NP, TMP solution and FA-CS-NP with doses equal to FA-TMP-NP IC_{95} was used as control preparations and verapamil solution (10 μg·mL^{-1}) was used as positive control. Cells were incubated at 37°C in a 5% CO_2 humid environment for 24 h. 0.5% MTT (Sigma, America) solution was added to each well and incubated for another 4 h. Then, 100 μL DMSO was added into each well and the absorbance was detected by microplate reader at 492 nm. The cell viability of each group was calculated.

ADM accumulation assay

To determine the reversal effect of MDR by FA-TMP-NP, ADM accumulation assay was performed on flow cytometer and laser scanning confocal microscope. MCF7/ADM and MCF-7 cells were seeded at a density of 2×10^6 mL^{-1} in 6-well plate. After treatment with ADM and FA-TMP-NP (IC_{95}), or control preparations for 24 h, the cultured cells were trypsinized and washed 3 times with cold PBS, harvested, and then resuspended with PBS. The fluorescence intensity was detected by flow cytometer with an excitation wavelength of 530 nm and an emission wavelength of 570 nm. In addition,

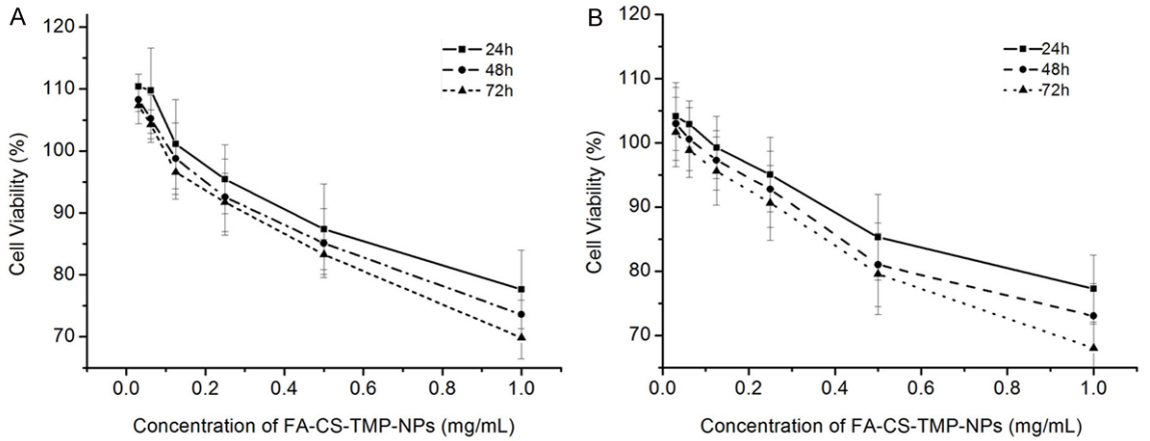

Figure 2. FA-TMP-NP alone slightly decreased the cell viability of both MCF-7/ADM K562/ADM cells. A: Cell viability of MCF-7/ADM cells treated with FA-TMP-NP for 24, 48 and 72 hr at the indicated concentrations; B: Cell viability of K562/ADM cells treated with FA-TMP-NP for 24, 48 and 72 hr at the indicated concentrations. Mean ± S.D., n=3.

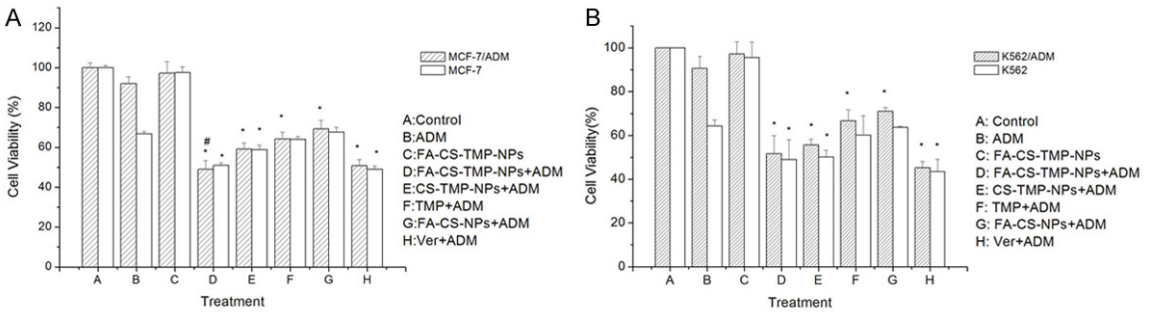

Figure 3. FA-TMP-NP sensitized both MCF-7/ADM and K562/ADM cells to ADM but not verapamil. A: Cell viability of MCF-7/ADM and MCF-7 cells treated with different drugs as indicated for 24 h; B: Cell viability of K562/ADM and K562 cells treated with different drugs as indicated for 24 h. *P<0.05 compared with group B, #P<0.05 compared with group E.

MCF-7/ADM and MCF-7 cells were seeded into a 24-well plate at a density of 2×10^6 mL^{-1}. After combination treatment for 24 h, cell morphology was photographed by a laser scanning confocal microscope.

Intracellular ADM concentration assay

MCF-7/ADM and MCF-7 cells were seeded into a 6-well plate at a density of 2×10^6 mL^{-1}. After treatment with ADM and FA-TMP-NP (IC_{95}), or control preparations for 24 h, the cells were collected, washed 3 times by PBS, dissolved in hydrochloric acid (3 $mol\cdot L^{-1}$) ethanol (60%) solution, and lysed by cell cracker. The supernatant was collected by centrifugation at 15000 RPM for 15 min. The fluorescence intensity of intracellular ADM was detected by fluorescence spectrophotography and drug concentration was calculated according to the linear regression equation.

Western blot

The cells were cultured and treated in the same condition as mentioned before. After exposure to drugs for 24 h, cells were washed 3 times with cold PBS and then lysed with RIPA lysis buffer (Beyotime Institute of Biotechnology, China) supplemented with 1 mM phenylmethylsulfonyl fluoride (PMSF). The protein concentration was determined by Bradford's protein assay. Protein samples were diluted in sample buffer (0.5 M Tris-HCl pH 6.8, 10% glycerol, 10% w/v SDS, 5% β_2-mercaptoethanol, 0.05% w/v bromophenol blue) and boiled for 3 min. 25 μg protein was separated by SDS-PAGE and transferred onto a nitrocellulose filter membrane. Membranes were blocked with 5% nonfat milk at 37°C for 2 hours, and incubated with rabbit monoclonal anti-human P-gp (1:200), mouse monoclonal anti-human GST-π (1:1000),

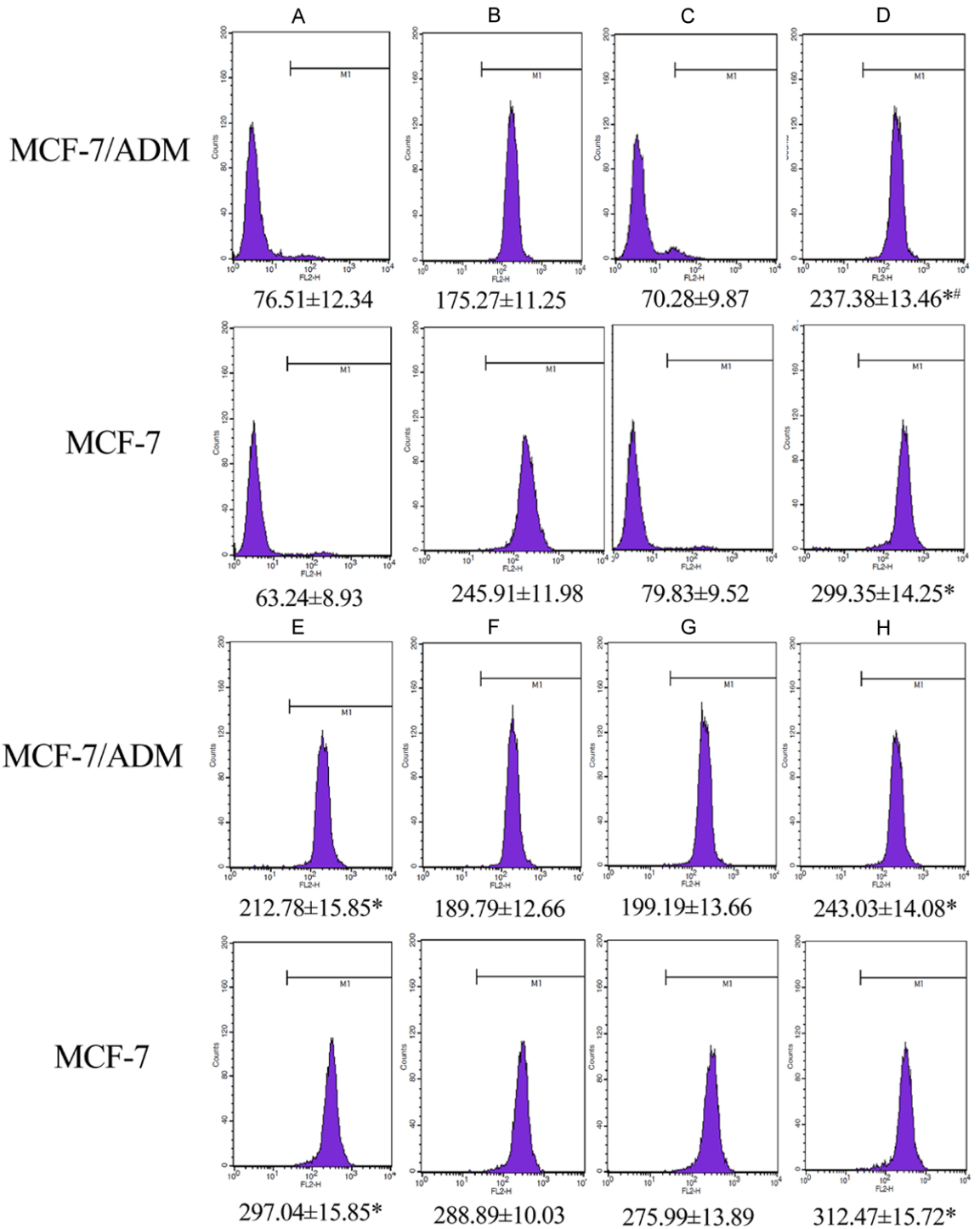

Figure 4. Intracellular fluorescence of ADM in MCF-7/ADM and MCF-7 cell lines detect by FCM ($\bar{X}$±S, n=3). A: Control; B: ADM; C: FA-CS-TMP-NPs; D: FA-CS-TMP-NPs+ADM; E: CS-TMP-NPs+ADM; F: TMP+ADM; G: FA-CS-NPs+ADM; H: ver+ADM. *P<0.05 compared with group B; #P<0.05 compared with group E.

or β-actin (1:1000) antibodies overnight at 4°C, followed by incubation with horseradish peroxidase-labeled goat-rabbit or goat-mouse immunoglobulin G (1:5000). Signals were developed by ECL substrate (Amersham, UK). Experiments were repeated for 3 times.

Real-time PCR

Cells were washed 3 times with cold PBS after 24 h incubation with drugs, and then total RNA was extracted by RNAiso plus (TaKaRa, Dalian, China) according to the instructions and quantified by spectrophotometer. cDNA was synthesized using TaKaRa Master Mix (SYBER Green) kit at 37°C for 15 min and 85°C for 5 sec. The sequences of the primers for MDR-1, GST-π and β-actin were shown in **Table 1**. Real-time PCR reactions were performed on the ABI PRISM® 7500 Real-Time Systerm by the following conditions: denature at 95°C for 5 sec, followed by 40 cycles at 95°C for 5 sec, 55°C for 30 sec and 72°C for 1 min. The PCR products were subjected to a melting curve analysis to confirm specificity of amplification. Experiments were repeated for 3 times.

Statistical analysis

Statistical analysis was performed by SPSS 11.5 software. Data were shown as mean ± SD. The differences between groups were compared by One-Way ANOVA, and the Normality test and Homogeneity test of variance were used to check the applicability of the data. LSD and S-N-K method were used to test the differences between any two groups. $P< 0.05$ was considered statistical significance.

Results

Characterization of FA-TMP-NP

TEM analysis of FA-TMP-NPs morphology revealed that they formed uniform spherical nanoparticles (**Figure 1**). Dynamic light scattering assay indicated that the average size of the NPs was 182.7±0.56 nm and their polydispersity index was 0.173, which was relatively low, demonstrating the narrow particle size distribution. The EE and LE were estimated to be 59.6±0.23% and 15.3±0.16%, respectively.

Cytotoxicity assay result

To investigate the toxicity of FA-TMP-NP treatment on MCF-7/ADM and K562/ADM cells, we measured the cell viability by MTT. FA-TMP-NP slightly decreased the viability of both MCF-7/ADM and K562/ADM cells with the increase of time (24-72 h) and concentration (31-1000 $\mu g \cdot mL^{-1}$). After 24 h, the IC_{95}, IC_{85} and IC_{80} in MCF-7/ADM cells were 0.261 $mg \cdot mL^{-1}$, 0.503 $mg \cdot mL^{-1}$ and 0.737 $mg \cdot mL^{-1}$, respectively (**Figure 2A**). The IC_{95}, IC_{85} and IC_{80} in K562/ADM cells exposed to FA-TMP-NP for 24 h were 0.238 $mg \cdot mL^{-1}$, 0.481 $mg \cdot mL^{-1}$ and 0.704 $mg \cdot mL^{-1}$, respectively (**Figure 2B**). The results demonstrated that FA-TMP-NP at all tested concentrations showed no obvious toxic effect on cellular viability.

FA-TMP-NP sensitizes MCF-7/ADM cells to ADM

To study the MDR reversal influence of FA-TMP-NP on MCF-7/ADM cells, we determined the cytotoxicity of ADM in presence or absence of FA-TMP-NP by MTT assay. After exposure to a safe dose (IC_{95}) of FA-TMP-NP in combination with ADM for 24 h, the growth rate of MCF-7/ADM was dramatically decreased. Moreover, there was statistically significant difference of cell growth between CS-TMP-NPs and TMP treated cells (**Figure 3A**). However, when the same treatments were conducted in K562/ADM cells, which express very low FR, there was no statistical difference in growth inhibition between FA-TMP-NP+ADM and CS-TMP-NPs+ADM (**Figure 3B**). Moreover, no statistical significant difference of cell growth was found between FA-TMP-NP+ADM and Verapamil+ADM in both cell lines (**Figure 3**).

FA-TMP-NP increases the cellular uptake of ADM

The result of flow cytometer analysis was shown in **Figure 4**. In contrast to ADM group, the increase of cell fluorescent intensity could be observed in both active and passive targeting groups. However, the increase level of active group was significantly higher than that of the passive preparation. Moreover, there was no obvious difference between the active targeting group and Verapamil+ADM group. Laser scanning confocal microscope indicated the same result as flow cytometer analysis (**Figure 5**). FA-TMP-NP could significantly increase intracellular uptake of ADM.

FA-TMP-NP increases the intracellular concentrations of ADM

To further investigate the reversal influence of FA-TMP-NP on MCF-7/ADM cells, we determined the intracellular ADM concentrations by fluorescence spectrophotography detection. After 24 h incubation, the intracellular ADM

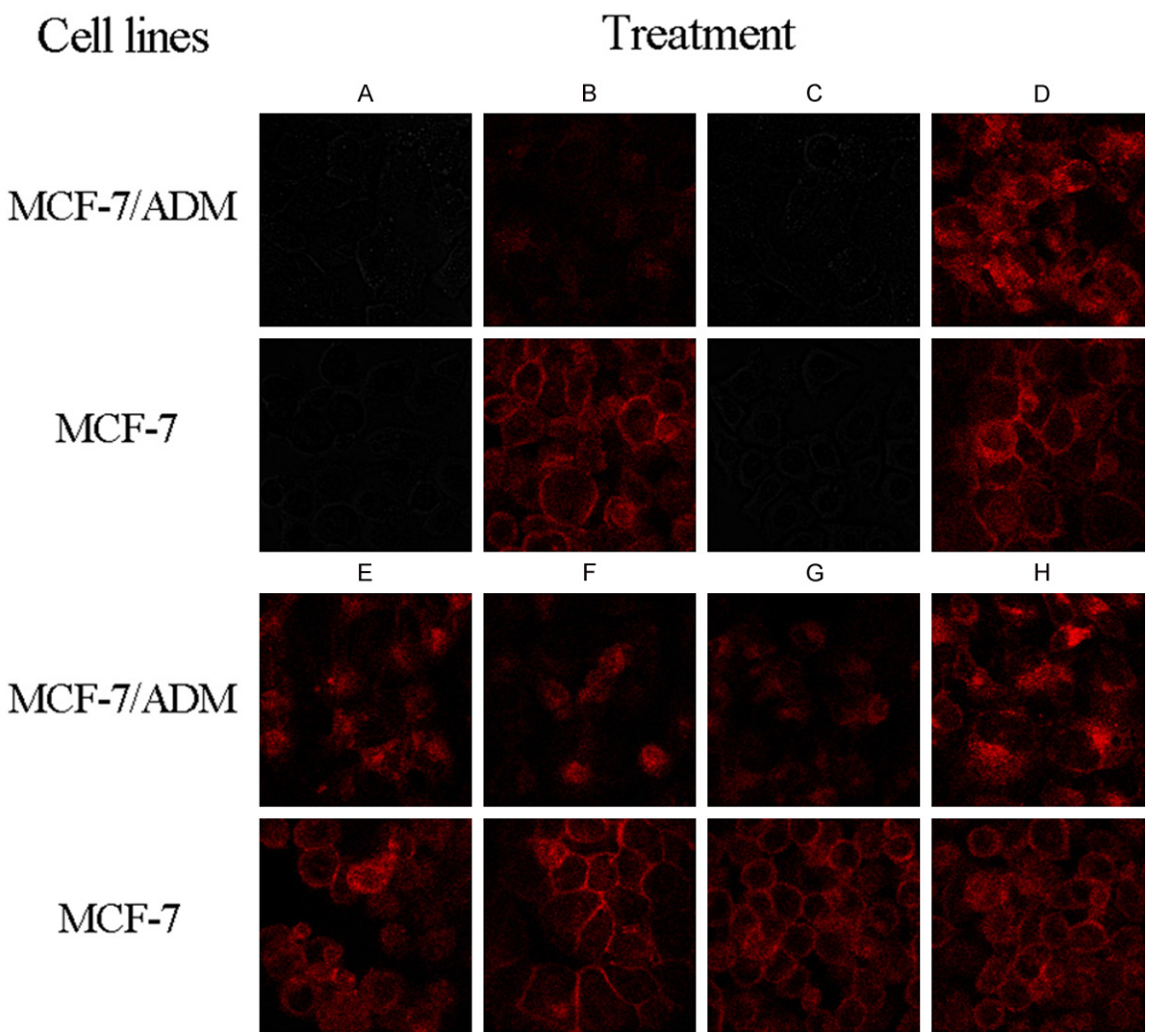

Figure 5. Accumulation of ADM detected by laser confocal microscope. A: Control; B: ADM; C: FA-CS-TMP-NPs; D: FA-CS-TMP-NPs+ADM; E: CS-TMP-NPs+ADM; F: TMP+ADM; G: FA-CS-NPs+ADM; H: ver+ADM.

concentration was 0.343±0.013 μg·mL^{-1} without combining reversal agent. In constrast, the concentrations were 0.716±0.016 μg·mL^{-1} and 0.630±0.036 μg·mL^{-1} when combined with active targeting or passive targeting nanoparticles groups, respectively (**Figure 6**). Compared with ADM group, both active and passive targeting nanoparticles increased the intracellular concentrations of ADM. Moreover, in comparison to passive targeting nanoparticles, active targeting nanoparticles significantly increased the intracellular ADM concentration.

To further investigate the dynamics of the FA-CS-TMP-NP-mediated increase in intracellular ADM, we treated MCF-7/ADM cells with different concentrations of FA-TMP-NP over time. Within 24 h, the concentration of intracellular ADM in MCF-7/ADM cells was dramatically increased with the increase of administration dose and incubation time, indicating that the reversal effect of FA-TMP-NP is time and concentration dual-dependent. Moreover, the concentrations of three groups all became stable after 24 h, suggesting that time-dependent ceases once cellular uptake reaches equilibrium. Therefore, the increase of intracellular ADM relies on both the treatment time and its concentration (**Figure 7**).

FA-TMP-NP decreases the expression of P-gp and GST-π

P-gp and GST-π are widely used as MDR markers. We used these markers to evaluate whether or not FA-TMP-NP can reverse MDR. In this study, we compared the changes of pro-

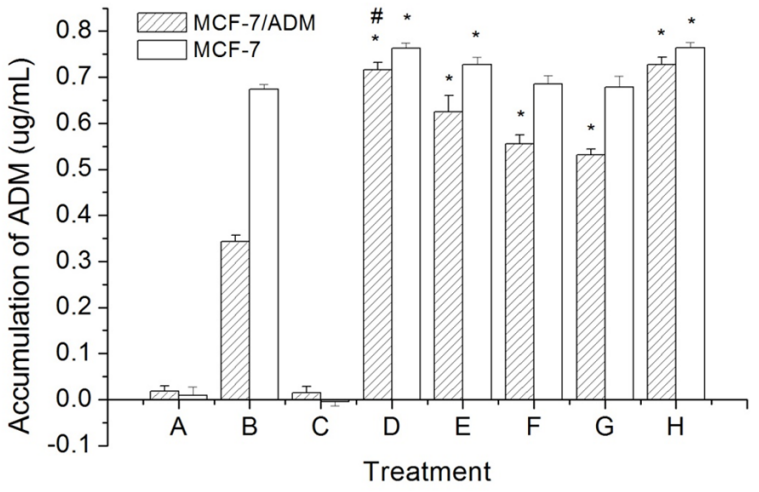

Figure 6. Accumulation of intracellular ADM in MCF-7/ADM and MCF-7 ($\bar{x}$ ±S, n=3). A: Control; B: ADM; C: FA-CS-TMP-NPs; D: FA-CS-TMP-NPs+ADM; E: CS-TMP-NPs+ADM; F: TMP+ADM; G: FA-CS-NPs+ADM; H: ver+ADM. *P<0.05 compared with Group B; #P<0.05 compared with group E.

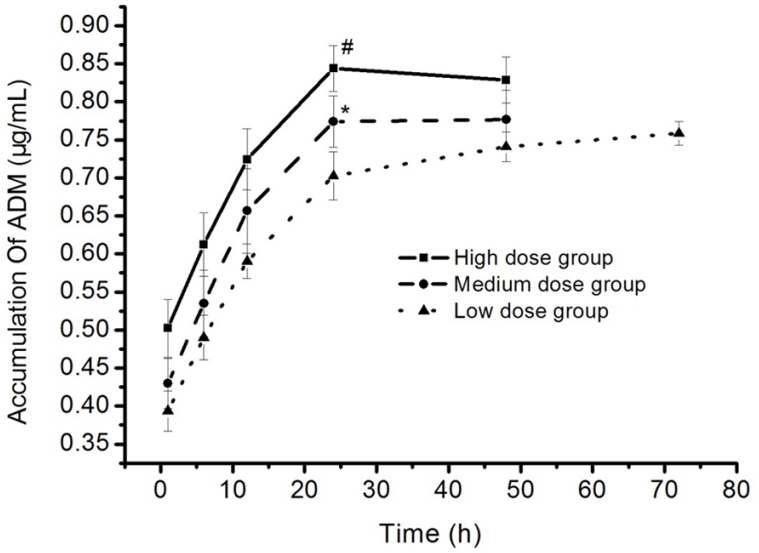

Figure 7. Accumulation of intracellular ADM in different time with different dose of FA-CS-TMP-NPs ($\bar{x}$ ±S, n=3). *P<0.05 compared with low dose group; #P<0.05 compared with medium dose group.

tein level of P-gp and GST-π between the control groups and the groups treated with FA-TMP-NP for 24 h. As shown in **Figure 8**, the expression level of P-gp and GST-π by FA-TMP-NP was significantly lower than that of by CS-TMP-NPs (**Figure 8A** and **8B**). In consistence, FA-TMP-NP significantly downregulated the mRNA levels of MDR-1 and GST-π in comparison to controls (**Figure 8C** and **8D**).

Discussion

In this study, we have investigated the ability of FA-TMP-NP to reverse cancer multidrug resistance *in vitro* and explored the potential underlying mechanism. We used folate receptor overexpressing cell lines MCF-7/ADM and MCF-7 as the experimental groups, and the cell lines K562/ADM and K562 with reduced expression of folate receptor served as the control group. We defined FA-TMP-NP as active targeting nanoparticles and CS-TMP-NP as passive targeting nanoparticles. Our results showed that there was a significant difference of the reversal effects between active and passive targeting nanoparticles. Although both nanoparticles could improve the sensitivity of MCF-7/ADM and MCF-7 to chemotherapy, there was significant difference between active nanoparticles and passive nanoparticles. The effect of the active targeting nanoparticles was significantly stronger than the passive preparation. However, in K562/ADM and K562 cells, no significant differences were observed between active nanoparticles and passive nanoparticles. These results indicated that active nanoparticles exert a superior reversal effect in MDR cells with high expression of folate recptor, suggesting that FA-TMP-NP holds great promise for the treatment of cancers.

The molecular mechanism that TMP reverses MDR is largely unknown so far. Recently, it has been shown that TMP can block calcium channels, suggesting that TMP may suppress drug export in cancer cells [16]. In this study, we found that TMP apparently downregulated the

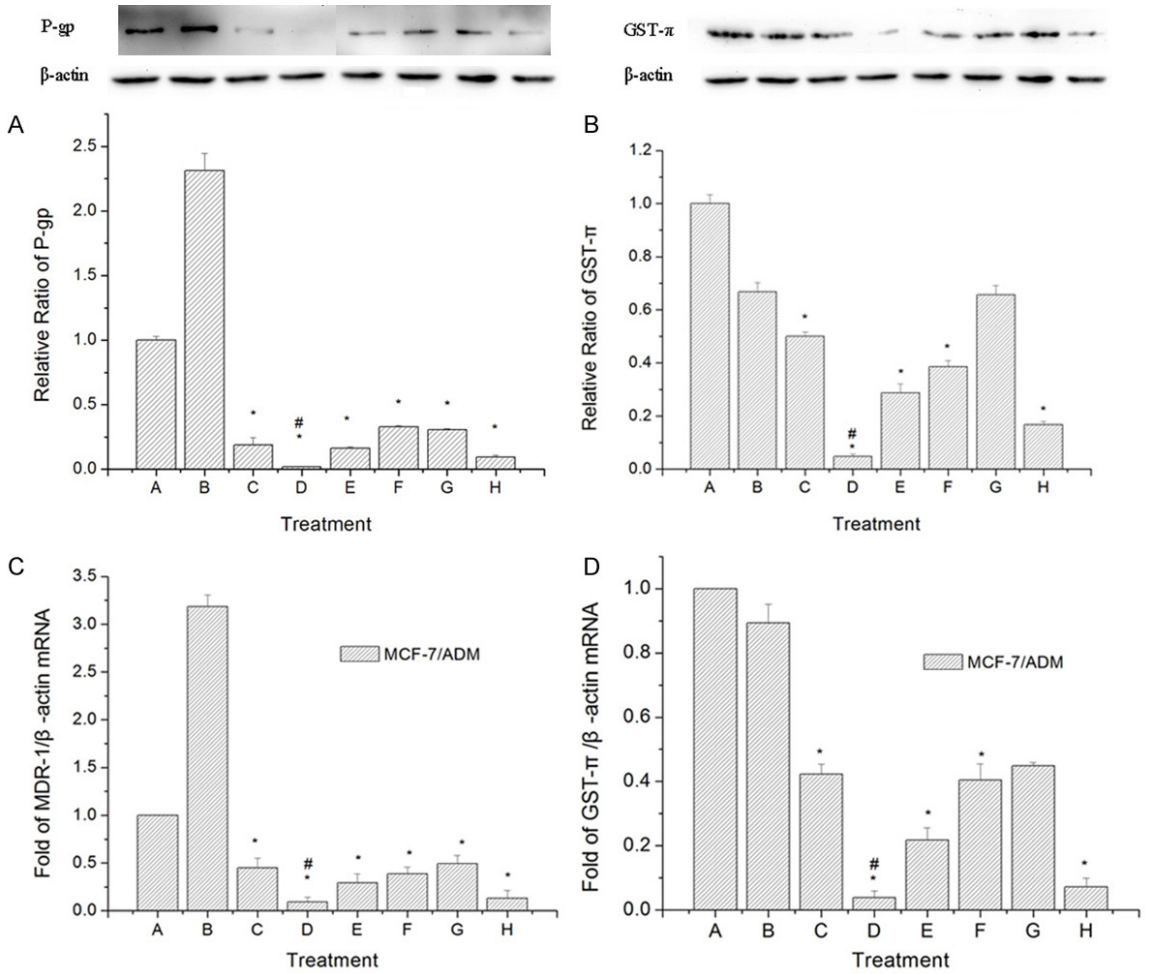

Figure 8. FA-TMP-NP decreased the expression of P-gp, GST-π and MDR-1. A. Protein level of P-gp determined by Western blots (mean ± S.D., n=3); B. Protein level of GST-π as determined by Western blots (mean ± S.D., n=3); C. mRNA level of MDR-1 determined by real time RT-PC (mean ± S.D., n=3); D. mRNA level of GST-π determined by real time RT-PC (mean ± S.D., n=3). A: Control; B: ADM; C: FA-TMP-NP; D: FA-TMP-NP+ADM; E: CS-TMP-NPs+ADM; F: TMP+ADM; G: FA-CS-NPs+ADM; H: ver+ADM. *P<0.05 compared with Group B; #P<0.05 compared with group E.

expression of P-gp, accompanied with decreased MDR-1, which indicates that TMP may reverse MDR by decreasing the activity of ATP-dependent ABC transporter. In addition, TMP could reduce the expression of GST-π by gene suppression, suggesting an alternative reversal MDR approach by inhibiting detoxification.

Although verapamil plays a crucial role in reversing multi-drug resistance, but the side effects and great impact on the metabolism of anticancer drugs restricts its application in clinic. FA-TMP-NP may break this limitation owning to its great reversal effect, which can be developed in cancer therapy.

In summary, we have demonstrated that FA-TMP-NP could enhance the accumulation of ADM in overexpressing MDR cells *via* folate receptor-mediated endocytosis. Our results indicate that FA-TMP-NP is a novel drug delivery system, which could improve the specificity of tumor cells with high folate receptor expression to chemotherapy, suggesting promising further development as a reversal agent of MDR.

Acknowledgements

This work was supported by the Science and Technology Planning Project of Liaoning Province, China (grant No. 2012225020).

Disclosure of conflict of interest

None.

Abbreviations

MDR, multidrug resistance; TMP, tetramethylprazine; FA-TMP-NP, folate-modified chitosan nanoparticles loaded with TMP; CS-TMP-NP, chitosan nanoparticles loaded with TMP; FA-CS-NP, empty folate-modified chitosan nanoparticles; ADM, adriamycin; P-gp, P-glycoprotein; GSTs, glutathione S-transferases; MCF-7, human breast carcinoma cell line; MCF-7/ADM, multidrug resistance sub-line of MCF-7; K562, human leukemia cells; K562/ADM, multidrug resistance sub-line of K562; Ver, verapamil.

Address correspondence to: Qing Fan, Department of Pharmacy, The Second Hospital of Dalian Medical University, Dalian 116027, China. Tel: +86-0411-84670304; Fax: +86-0411-84670304; E-mail: fq731@sina.com

References

[1] Krishna R and Mayer LD. Multidrug resistance (MDR) in cancer. Mechanisms, reversal using modulators of MDR and the role of MDR modulators in influencing the pharmacokinetics of anticancer drugs. Eur J Pharm Sci 2000; 11: 265-283.

[2] Colabufo NA, Contino M, Berardi F, Perrone R, Panaro MA, Cianciulli A, Mitolo V, Azzariti A, Quatrale A and Paradiso A. A new generation of MDR modulating agents with dual activity: P-gp inhibitor and iNOS inducer agents. Toxicol In Vitro 2011; 25: 222-230.

[3] Miri R and Mehdipour A. Dihydropyridines and atypical MDR: a novel perspective of designing general reversal agents for both typical and atypical MDR. Bioorg Med Chem 2008; 16: 8329-8334.

[4] Shuker N, Bouamar R, Weimar W, van Schaik RH, van Gelder T and Hesselink DA. ATP-binding cassette transporters as pharmacogenetic biomarkers for kidney transplantation. Clin Chim Acta 2012; 413: 1326-1337.

[5] Susa M, Iyer AK, Ryu K, Choy E, Hornicek FJ, Mankin H, Milane L, Amiji MM and Duan Z. Inhibition of ABCB1 (MDR1) expression by an siRNA nanoparticulate delivery system to overcome drug resistance in osteosarcoma. PLoS One 2010; 5: e10764.

[6] Xu HB, Xu LZ, Li L, Fu J and Mao XP. Reversion of P-glycoprotein-mediated multidrug resistance by guggulsterone in multidrug-resistant human cancer cell lines. Eur J Pharmacol 2012; 694: 39-44.

[7] Burg D, Filippov DV, Hermanns R, van der Marel GA, van Boom JH and Mulder GJ. Peptidomimetic glutathione analogues as novel γGT stable GST inhibitors. Bioorg Med Chem 2002; 10: 195-205.

[8] Dačević M, Isaković A, Podolski-Renić A, Isaković AM, Stanković T, Milošević Z, Rakić L, Ruždijić S and Pešić M. Purine Nucleoside Analog-Sulfinosine Modulates Diverse Mechanisms of Cancer Progression in Multi-Drug Resistant Cancer Cell Lines. PLoS One 2013; 8: e54044.

[9] He L and Liu GQ. Effects of various principles from Chinese herbal medicine on rhodamine123 accumulation in brain capillary endothelial cells. Acta Pharmacol Sin 2002; 23: 591-596.

[10] Yang XG and Jiang C. Ligustrazine as a salvage agent for patients with relapsed or refractory non-Hodgkin's lymphoma. Chin Med J (Engl) 2010; 123: 3206.

[11] Sau A, Pellizzari Tregno F, Valentino F, Federici G and Caccuri AM. Glutathione transferases and development of new principles to overcome drug resistance. Arch Biochem Biophys 2010; 500: 116-122.

[12] Qing F, Guangjun F, Jinyao Z and Peiman Y. Study on Effect Reversing MDR of Ligustrazine Liposomes on Human Erythroleukemia cell line K (562)/ADM. China Pharmacist 2004; 10: 003.

[13] Lu YG, Sun QR, Zhang M, Wang QH and Wang BF. Intensifying action of tetramethylpyrazine on ADR-resistent hepatocellular carcinoma cells. Chinese Journal of Integrated Traditional and Western Medicine on Digestion 2013; 6: 005.

[14] Wang XB, Wang SS, Zhang QF, Liu M, Li HL, Liu Y, Wang JN, Zheng F, Guo LY and Xiang JZ. Inhibition of tetramethylpyrazine on P-gp, MRP2, MRP3 and MRP5 in multidrug resistant human hepatocellular carcinoma cells. Oncol Rep 2010; 23: 211-215.

[15] Shen Z, Li Y, Kohama K, Oneill B and Bi J. Improved drug targeting of cancer cells by utilizing actively targetable folic acid-conjugated albumin nanospheres. Pharmacol Res 2011; 63: 51-58.

[16] Chai S, To KK and Lin G. Circumvention of multi-drug resistance of cancer cells by Chinese herbal medicines. Chin Med 2010; 5: 26.